Diffusive hydrogen inter-cage migration in hydrogen and hydrogen-tetrahydrofuran clathrate hydrates

Huayu Cao[1], Niall J. English[1,2,a)] and J.M.D. MacElroy[1,2,b)]

[1]The SFI Strategic Research Cluster in Solar Energy Conversion, School of Chemical and Bioprocess Engineering and [2]Centre for Synthesis and Chemical Biology, University College Dublin, Belfield, Dublin 4, Ireland.

Keywords: Molecular Dynamics, Hydrogen Hydrate, THF Hydrate, Diffusion, Migration, Fickian

Classical equilibrium molecular dynamics (MD) simulations have been performed to investigate the diffusive properties of inter-cage hydrogen migration in both pure hydrogen and mixed hydrogen-tetrahydrofuran sII hydrates at 0.05 kbar from 200 K and up to 250-260 K. For mixed H_2-THF systems in which there is single H_2 occupation of the small cage (labelled '1SC 1LC'), we found that no H_2 migration occurs. However, for more densely-filled H_2-THF and pure- H_2 systems, in which there is more than single H_2 occupation in the small cage, there is an onset of inter-cage H_2 migration events from the small cages to neighbouring cavities at around 200 K. The mean square displacements of the hydrogen molecules were fitted to a mathematical model consisting of an anomalous term and a Fickian component, and non-linear regression fitting was conducted to estimate long-time (inter-cage) diffusivities. An approximate Arrhenius temperature relationship for the diffusion coefficient was examined and a rough estimation of the hydrogen hopping energy barrier was calculated for each system.

[a,b)] Corresponding authors. Tel: +353-1-716-1646 (N.E.), 1824 (J.M.D. MacE). Email: niall.english@ucd.ie, don.macelroy@ucd.ie

INTRODUCTION

Gas hydrates are crystalline inclusion compounds wherein a water lattice forms a periodic array of cages, with each cavity sufficiently large to contain one, or possibly more, gas molecules [1,2]. Given our interest in hydrogen and tetrahydrofuran sII hydrates in this study, a unit cell in sII [3] hydrate consists of 136 water molecules forming sixteen small cages and eight large cages. The small cages are pentagonal dodecahedral in nature (5^{12}), whilst the large cages are hexacaidecahedral ($5^{12}6^4$).

Possible exploitation of sII hydrates for hydrogen storage has been studied extensively [5-7]. Mao *et al* found that at pressure 200 MPa, hydrogen and water mixtures crystallise in the form of sII clathrate, and that at a pressure of 180-220 MPa and 300 K, the experimentally determined guest-to-H_2O molecular ratio is 0.45±0.05. It indicates the multiple occupations in the small and large cages. This value is within the error of the theoretical value of 0.47, which indicates that small cages are doubly and large cages are quadruply occupied [4] under high-pressure conditions. Therefore, across a broader pressure range, each 5^{12} cage may contain one, or possibly two, H_2 molecules, while each $5^{12}6^4$ cage may contain a single THF molecule or up to four H_2 molecules [4]. The extreme pressure needed for formation of pure hydrogen hydrate has been a limiting factor and has led to the study of mixed stabiliser-H_2 hydrates [8,9,10], in the hope that a stabilising compound will allow hydrate formation at lower pressures. Hydrates stabilised by THF have attracted interest in this respect as they have been reported to be stable at close to room temperature, and at much lower pressures than pure hydrogen-hydrate [4,5,8,11]. For instance, Florusse *et al* showed that the clathrate can be stabilised with the large cage singly occupied by a second guest molecule component, tetrahydrofuran (THF) at a lower pressure of 5 MPa and a higher temperature 279.6 K. Lee *et al* [8] used Raman spectroscopy to discover that in binary hydrates of THF and hydrogen, in which the mole ratio of THF was 5.6%, the small cavities were occupied by two hydrogen molecules. At a pressure of 15 MPa and a temperature of 270 K, the hydrogen mole ratio was found to increase to 4% with a THF mole ratio of 0.15% [8]. By tuning the composition of THF in the

binary clathrate, the hydrogen storage capacity could be altered and controlled [8], which is a promising development for hydrogen storage.

Although the concept of large-scale seasonal storage is not new [12], the proposal of using mixed THF-H_2 hydrate for such efforts [13] is attractive, as it is a completely reversible physical hydrogen storage material. However, the exact weight percentage of hydrogen in such a system is still disputed, with estimates ranging from 1-4 wt% H_2 [8,13] affecting its viability as a storage medium substantially. It is understood that hydrate structures which enable multiple occupancy of hydrogen will likely be required for clathrate hydrate to be a practical hydrogen storage medium. Nakayama *et al* [14] present part of a Tokyo-based feasibility study of large-scale *in situ* storage of hydrogen in the form of clathrate hydrates, in which it is concluded that a large portion of the energy which could be extracted from hydrogen hydrate would be needed to power the necessary refrigeration. However, their industrial design does not address the possibility of the seasonal, geologic storage of hydrates, *i.e.*, possible storage in large-scale underground caverns where lower temperatures may be achieved at a lower energy cost, for seasonal physical storage and reversible release [14].

Given that pressure plays an important role in the occupancy of the cavities, it is to be expected that triple occupancy of small cages may require extremely high pressure. It has been reported by Rovetto *et al* that only single occupancy in the small cavity of sII clathrate was observed at 70 MPa and 20 K [15]. This indicates that single occupancy in the small cages is much more likely than the double occupancy. As Nakayama *et al* concluded, the high pressures required for large-scale hydrogen storage would not be economically feasible [14]. Bearing these points in mind, a study of differing average small-cage compositions would seem to be of benefit (*i.e.*, varying proportions of singly- and doubly-occupied small cavities), and we have performed equilibrium molecular dynamics (MD) simulations in this work to probe and model the hydrogen diffusion process between cavities of pure- and mixed-hydrogen clathrates for varying degrees of occupation of the small cavities.

Previous applications of MD and molecular simulation to study guest-diffusivity in clathrates, as

well as experimental guest-diffusivity data, and the modelling of such diffusion in heterogeneous media in general, are of direct relevance to this study. Peters *et al* have studied methane diffusivity in hydrates via a path-sampling method [16]. Moreover, Demurov *et al* have studied CO_2 migration and the energy barriers and rates for hopping events were calculated by Monte Carlo simulations [17]. At the same time, several workers have investigated hydrogen hopping via molecular simulation. Alavi and Ripmeester [18, 19] have observed hydrogen migration energy barrier through electronic structure and diffusion pathways based on four different configurations of hydrogen molecules within small cages, *i.e.*, either parallel or perpendicular to the pentagonal or hexagonal face. The rate of H_2 migration and the self-diffusion coefficient were plotted against temperature for the four different configurations, which indicates that the hydrogen migration frequency increases with temperature, as measured by its self- diffusion coefficient. Moreover, Frankcombe and Kroes [20] observed hydrogen migration via MD. They discovered that hydrogen migration did not occur from singly-occupied small cages; it appeared that traversing through the pentagonal face of the small cage is a formidable challenge in the time range simulated. Even though the interactions between H_2 may lead to high energy barrier, such resistance was not found to be prevalent when a hydrogen molecule moves from one cage to another with low occupancy [20]. This implies that the H_2-$(H_2O)_5$ energy barrier inhibits hydrogen hopping. However, occupation of up to six hydrogen molecules in a large cage was observed by Frankcombe and Kroes, with lifetimes of up to hundreds of picoseconds [20]. In addition, Gorman *et al* [21] have studied hydrogen migration in clathrates, with a similar lack of observations of hopping in systems with singly-occupied small cavities. Nevertheless, hydrogen migration was detected in doubly occupied systems, with H_2 motion transverse to the pentagonal face into the neighbouring cages. Occasionally, the hydrogen which moves to the surface of the small cage may stay for a couple of picoseconds, weakening the stabilising hydrogen bonds of the five-membered water ring, *i.e.*, the pentagonal surface. This allows a temporary channel to open for the hydrogen molecule, which results in the hydrogen hopping.

Experimental studies into hydrogen migration in clathrates also offer interesting insights, particularly to estimate the diffusivity of hydrogen within binary hydrogen-THF hydrates. Saha and Deng have found that the diffusivity of hydrogen is on the order of 10^{-18}-10^{-19} m^2/s at 270 K and 65 bar [22]. However, Okuchi *et.al* have used high-pressure diamond anvil cell NMR to measure the diffusivity of hydrogen at 3.6 GPa and 291 K, and found that the diffusivity was up to 2×10^{-9} m^2/s, with little pressure sensitivity, which is indicative of liquid-like diffusion behaviour [23]. Senadheera and Conradi [24] found that their NMR line-shape results for enclathrated H_2 motion appeared to suggest larger energy barriers during inter-cage hopping (~27 kcal/mol), which is inconsistent with what Okuchi *et al* observed in TDF/H_2 D_2O clathrates (0.48-0.96 kcal/mol) [25]. Senadheera and Conradi [24] found their results were more compatible with experimental data of hydrogen diffusion observed by Mulder *et al* [26].

Given our interest in developing descriptive quantitative models for the underlying hydrogen-transport processes, focussing on anomalous cage-hopping and the consequent development of Fickian diffusion, it is appropriate to consider briefly previous work on such models in heterogeneous media, wherein one phase, composed of nanoscale 'super-conducting' domains (akin to cavities in hydrates), is dispersed in another, with hopping between the dispersed phase domains. McDermott *et al* [27] have developed a mathematical model to explain the self-diffusion behaviour of helium and other gases in discontinuous channels in nano-porous, ultra-thin, dense silica films, with an anomalous term and a Fickian component. The anomalous term represents 'super-conducting' diffusion (i.e., within the dispersed domains, or cages in the case of hydrates), while the Fickian term represents diffusion in the slower, continuous medium (akin to hopping between cavities in hydrates). Experimentally, the super-conducting domains consist of pores with characteristic dimensions of the order of 1 nm or less. Silica films with a thickness of 30-100 nm accommodate these pores [28-30]. The gas molecules were found to selectively permeate thin film membranes via these pores, competing, in parallel, with Fickian transport in the poorly-diffusing domain [27].

This study seeks to develop such a mathematical model for hydrogen diffusion in hydrates, to model the 'anomalous' (intra-cage) and Fickian (inter-cavity) self-diffusion process. We wish to study the influence of temperature and the hydrogen occupation of the small cavities (i.e., governed by the ratio of singly- to doubly-occupied cavities – varying this ratio for different overall small-cavity occupations). Rovetto et al [15] found that triple occupancy is unlikely, and we only observed transient instances of this in previous work [21]. Therefore, we have carried out equilibrium MD at 50 bar, of interest to industrial storage, and from 200 up to 260 K for different small-cage hydrogen occupancies, including both pure and mixed THF-H_2 clathrates, and we have applied the anomalous-Fickian diffusion-modelling approach of McDermott *et al* [27] to further characterise and quantify the inter-cage hopping diffusion rates observed in our previous study [21], and ascertain thereon the effect of small cage H_2 occupancy.

METHODOLOGY

Molecular Dynamics

An sII hydrate supercell, consisting of 2×2×2 unit cells, was constructed; the unit cell length was 17 Å [3]. The Bernal-Fowler rules were employed to choose the initial orientation of the water molecules [31], minimising the total dipole moment. In addition, the Rahman-Stillinger procedure was also used to render the total dipole moment vanishingly small [32]. Ten systems were constructed, five of pure hydrogen hydrates and five mixed (THF-H_2) systems. These systems and naming conventions are further described in Table I below – essentially, the ratio of singly- to doubly-occupied small cages was varied to achieve a range of overall average small cage occupations between 1 and 2. The guest molecules' initial positions were chosen by placing the centre of mass (COM) of THF at the geometric centre of large cage. If the small cage is doubly occupied by two hydrogen molecules, they are reasonably arranged at energetically stable positions relative to one another and the cage wall, while single-occupation entailed placing the COM of H_2 at the geometric centre of small cages.

[insert Table I about here]

TIP4P-2005 was chosen as the water model, due to its reasonable performance for a variety of properties, including thermodynamic properties of the liquid and solid phases, properties at melting and vaporisation points etc, covering a wide temperature (from 123 to 573 K) and pressure range (up to 40,000 bar) [33]. For THF and H_2, we used the Lennard-Jones (LJ) parameters and charges of Alavi *et al* [34]. Geometric combining rules were used for cross water-H_2 and water-THF LJ interactions, *i.e.*, $\varepsilon_{ij}^0 = \left(\varepsilon_{ii}^0 \varepsilon_{jj}^0\right)^{0.5}$, $\sigma_{ij}^0 = \left(\sigma_{ii}^0 \sigma_{jj}^0\right)^{0.5}$, where ε and σ have their usual meanings. DL-POLY 2 [35] was used to carry out equilibrium classical MD [36] simulations. It should be pointed out that the use of classical MD to treat hydrogen molecules' motion, in particular, below around 150 K is approximate in nature, and the lack of provision of quantum effects like zero-point H_2 cage-rattling motions and quantisation of H_2 rotational motion becomes less satisfactory at lower temperature. However, given that this study focuses on hydrogen transport phenomena at and above 200 K, the use of classical MD is reasonably justified. Long-range electrostatic interactions were computed on the basis of the Smoothed Particle Mesh Edward (SPME) method [37] and the cut-off distance of van der Waals interactions and real-space electrostatics was 10 Å. In the SPME method, the screening parameter, α, and the number of wave-vectors were arranged so that the relative error was less than 1×10^{-5}; the Ewald electrostatic energy and forces changed little with α. Rigid molecule models were employed for H_2, THF and H_2O with the NOSQUISH algorithm of Miller *et al*. [38], using velocity-Verlet [39] integration. 100 ps of Nosé-Hoover [40] NVT simulations were run at 200, 220, 230, 240, 250, 260 K for each system with 2 fs time step at 0.05 kbar, and a rather mild 0.5 ps thermostat relaxation time; these were followed by 250 ps of NPT runs [41, 42] at 0.05 kbar at each temperature, with thermostat and barostat periods of 0.5 and 2 ps respectively, to allow each system volume to settle. NPT production runs, with the same thermostat and barostat periods, were performed on the relaxed systems for a further 2.5 ns with a 2 fs time-step at 0.05 kbar and

each temperature between 200 and 260 K. During the simulation, it was found that 2S4L was not stable at 250 K and 260 K, and 1.75S4L did not remain intact at 260 K. The presence of THF played an important role in stabilising the system, as observed by Frankcombe and Kroes [20].

Mathematical Modelling

The novel work of explaining the diffusion within ultrathin, dense silica films has been done by McDermott *et al* [27]. Occasionally, hydrogen molecules were found to jumps out of their cages and moves to neighbouring ones. The frequency of hydrogen hopping is not very high, so that energy barriers exist to impede the diffusion process, just like that observed in the poorly diffusing domain in the dense silica system simulated and modelled by McDermott *et al* [27]. It is reasonable to use an analogous approach to investigate the mechanism of diffusion within clathrate hydrates, because of the similarity between the two systems (short-ranged order but long-ranged disorder) and the resemblance of the transport process ('super-conducting' within cages and poorly-diffusing domain for inter-cavity hopping).

For short-to-intermediate time scales gas permeation within the dense amorphous media is dominated by anomalous diffusion within 'non-percolating superconducting' domains with the mean square displacement (MSD) of the centre of mass of the gas molecules modelled as a function of time, *t* [27], as shown below:

$$\left\langle \left|\Delta \mathbf{r}(t)\right|^2 \right\rangle = \frac{At^{2/d_w'}}{1 + (A/6\ell^2)t^{2/d_w'}} \qquad (1)$$

where d_w' is the fractal-dimension of the random walk undertaken by the molecule within the medium, ℓ is the characteristic average range of displacement, in one direction, of the molecule under non-percolating conditions, i.e., moving rapidly within the 'superconducting' pores (or,

indeed, within a clathrate's cavity). *A* is a parameter which has specific value at a given temperature and for different clathrate systems, and is simply be treated as a fitting coefficient [27].

In clathrate hydrates, the hydrogen molecules are confined either in the small cavities or large cages and their trajectory evolution (beyond the initial ballistic regime) is modelled by Eq. (1) at short-to-intermediate times. At long times, however, hydrogen hopping arises from diffusion from one cage to another, as energy barriers between cages are overcome. To represent this hopping mechanism, a Fickian diffusion term is needed, with self-diffusion coefficient *D*, and in this case the MSD is represented by

$$\left\langle \left|\Delta \mathbf{r}(t)\right|^2 \right\rangle = 6Dt \qquad (2)$$

Combining the anomalous and Fickian terms of eqns. (1) and (2) yields the total MSD as

$$\left\langle \left|\Delta \mathbf{r}(t)\right|^2 \right\rangle = \frac{At^{2/d_w'}}{1 + (A/6\ell^2)t^{2/d_w'}} + 6Dt \qquad (3)$$

Here, *D* is the long-time self-diffusion coefficient in the poorly conducting domain, representing a *de facto* rate generated by hopping events. As will be demonstrated below, this approach accurately models the MSD trajectories in each of the systems investigated here.

Inter-cage migration has been observed by Gorman *et al* [21], as shown by Figure 2 of that article [21], as well as by Frankcombe and Kroes [20]. In ref. 21, the hydrogen molecules were often observed to move to the pentagonal face of the small cage and then moved back to the geometric centre of the cage; this intra-cage, non-percolating movement occurred rapidly. Occasionally, the hydrogen molecule that moved to the surface of the small cage may weaken the stabilising hydrogen bonds, which may result in the temporary opening of the pentagonal face to allow the

hydrogen molecule to 'escape' from the cage. The rate of such hopping events was found to depend on temperature, and activation energies were estimated from approximate Arrhenius fits to hopping rates at different temperatures. One may characterise this general process in terms of an MSD as schematically illustrated in Fig. 1. At very short times, the H_2 molecules move within the cavities and the MSD is proportional to t^2 in the ballistic régime. However, for $t_\xi < t < t_x$, the MSD levels off at $6\ell^2$ in three dimensions; depending on the nature of the system, this approximate 'plateau' may be more or less pronounced. For $t > t_x$, the hydrogen diffuses (hops) and Fickian behaviour is observed.

[insert Figure 1 about here]

RESULTS AND DISCUSSION

Typical results for the MSDs for hydrogen (except 1S1L, which will be discussed later) within the stabilisation temperature range in this work are reported in Figs. 2 and 3. These MSDs were calculated from 2.5 ns simulation trajectories. A non-linear regression algorithm was used to compute the four parameters *A*, ℓ, $d_w^{'}$ and *D*, which appear in Eq. 3, from fitting of the MSDs between 10 to 500 ps. Non-linear regression was implemented via three different methods: Lsqcurvefit in MATLAB and Solver in Microsoft Excel (both of which, broadly, implement variations and improvements along the lines of the general Levenberg-Marquardt approach [43] to render this more robust, *vide infra*), and the SOLVOPT program which carries out the Shor algorithm [44]. Lsqcurvefit employs a subspace trust-region method based on the interior-reflective Newton method, as described by Coleman *et al* [45, 46]. During each iteration, this involves the approximate solution of a large linear system using the method of pre-conditioned conjugate gradients. In so doing, Lscurvefit inverts the variance/co-variance matrix Jacobian, and this can be combined with the appropriate *t*-distribution information to estimate 95%-confidence intervals for each of the four parameters in eqn. 3. The Generalised Reduced Gradient (GRG2) non-linear

optimisation [47] code is employed by Microsoft Excel's Solver function [48], although more problematic access to the variance-covariance matrix renders the estimation of confidence intervals with this implementation much more difficult; therefore, confidence intervals using Microsoft Excel have been omitted. The SOLVOPT program [49] was usually found to provide the tightest fit owing to the Shor algorithm [44], and the parameter values were more robust to changes in MSDs, echoing the findings of McDermott *et al* [27]; it was also possible to estimate confidence intervals with this approach. The results obtained from the three different approaches were found to be broadly consistent with each other, except for 1S4L system which required special fitting techniques, and where the SOLVOPT method was clearly superior.

[insert Figures 2 & 3 about here]

At the beginning of this fitting exercise, regression analysis involved all four parameters. However, the parameter values were quite scattered, especially that of the fractal-dimension parameter $d_w^{'}$, which was also observed by McDermott *et al* [27]. To achieve better fitting results and more consistent parameters, $d_w^{'}$ for diffusion in disordered system is known to be dependent on the nature of the bond connectivity and the uniformity of the media in three dimensions [50]. Although clathrate hydrates are ordered media for short-ranges, there is still long-range disorder. Generally, in disordered systems at intermediate times diffusion becomes anomalous

$$\left\langle \left|\Delta \mathbf{r}(t)\right|^2 \right\rangle \sim t^{2/d_w^{'}} \tag{4}$$

where $d_w^{'}$ is larger than 2 [50]. A rough estimation was conducted by measuring the slope of log-log plots of the MSD curves at intermediate times to estimate $d_w^{'}$. The value varied from 2.6 to 6.3. For

systems like clathrate hydrates, it is valid to assume the distribution is uniform in three dimensions. In this case, $d_w^{'}$ is limited by $3.49 < d_w' < 3.768$ [50]. On the basis of the observations from the approximate estimation of this parameter we believe it was suitable to fix $d_w^{'}$ at the value of 3.768, and this is consistent with the approach adopted by McDermott *et al* [27]. The resultant fitted parameters from SOLVOPT for *A*, *l* and *D* are provided in Tables II to IV, respectively, whilst the corresponding MATLAB Lsqcurvefit and Microsoft EXCEL results are provided in the Supplementary Information section [51].

[insert Tables I-IV about here]

Selected log-log MSD plots for the pure H_2 system, 2S4L, and for the mixed system, 2S1L, are reported in Figures 2 and 3. In all cases the transport of the hydrogen is non-Fickian (slope << 1 on the log-log plots) for much of the time up to 500 ps with the possible exception of the MSD over the time range 300-500 ps for the highest temperature simulation of the 2S4L system. Similar results were observed by McDermott *et al.* in the diffusion of helium within ultra-thin, dense nano-porous silica films [27]. However, in contrast to Helium which exhibited Fickian conditions over a much broader time range, in clathrate hydrates, where the hydrogen molecule may interact electrostatically with the surrounding water molecules forming the cages, the diffusion process may be weakened by Coulombic interactions and anomalous behaviour is therefore more significant. Gorman *et al.* have studied the energetics and dynamical properties of the guest (H_2)-water interactions [52]. Transitional, relatively short-lived hydrogen bonds formed between hydrogen molecules and the surrounding water molecules may explain this attraction, resulting in significant 'sub-Fickian' behaviour. The timescales required for the development of full Fickian diffusive behaviour, particularly at lower temperatures below the melting point, may be prohibitive for MD, and the use of specialised hardware for acceleration of hydrate-MD into micro- and even

millisecond times may be needed to achieve this [53].

An interesting contrast between the pure and mixed systems is demonstrated by considering the 1S4L(see Figure 4), 2S1L (see Figure 3) and 1S1L (Figure 5) simulation results. For the 1S4L system, the anomalous regime extends over a longer time period than for the 2S4L. This is not unexpected when the results for the 1S1L are taken into consideration. In the latter case there was no migration detected for the hydrogen molecules (See Figure 5). The single hydrogen molecule in the small cages in both systems 1S1L and 1S4L are largely non-percolating (as also observed in [21]). More vigorous vibration of the large cages due to quadruple occupation in the case of 1S4L, particularly at higher temperatures, coupled with single-occupation of the small cages allows for limited hopping to occur between small and large cages. In contrast, in the 1S1L system, the THF molecule stays in the large cage, and no hydrogen jumping was observed , with the *D* value vanishingly small.

[insert Figure 5 about here]

In order to show the fitting quality further, deconvolution of the anomalous term and Fickian terms was carried out. As shown in Figs. 6 and 7 for the 1.25S1L system at two extreme temperatures (200 K and 260 K), the magnitude of the two terms are similar and they make comparable contributions to the transport process during the sampling time.

[insert Figures 6 & 7 about here]

As mentioned earlier, the parameter ℓ is defined as the average range of displacement of the random walker (in this case, hydrogen) under non-percolating conditions, i.e., within the cages.

Below the transition temperature 250K, ℓ values calculated from the nonlinear regression vary from 0.403 to 0.917Å. Given that there are three types of cages available in the hydrogen hydrates: singly/doubly occupied cages and quadruple occupied large cavities, the ℓ value calculated should be the average range of displacement, in one direction, within the three types of cages. Notwithstanding this mixture of cell types, general trends can be observed. As the temperature is increased one would expect the cages to swell to some extent, particularly for those cells with high occupancy. This is clearly observed from the results in Table III. In the case of the 2S1L system, where the large cages are filled with non-diffusing THF molecules and the small cages are doubly occupied by hydrogen, the ℓ value represents the true maximum value under non-percolating conditions for the small cages. According to Gorman *et al* [21] the radius of the small cages in 2S1L ranges from 3.837-3.981 Å. If the plateau of the mean square displacement under 'non-percolating' condition,

$$\left\langle \left|\Delta \mathbf{r}(t)\right|^2 \right\rangle_{Max} = 6\ell^2$$

is physically taken to be the square of the distance a given hydrogen molecule can travel on average from the centre of the cage until it collides with the cage wall then the estimated value of ℓ for the 2S1L system assuming the cage is spherical, is

$$\ell \sim \frac{1}{\sqrt{6}}\left(R_{cage} - \sqrt{\sigma_{HH}\sigma_{OO}}\right) = 0.33\,\text{Å}$$

where the magnitude of the collision diameter of the hydrogen molecule and the water oxygen has been taken to be 0.3101 nm [7]. The larger values of ℓ reported in Table II are indicative of the atomic 'roughness' of the cage wall, dynamical fluctuations in the size and shape of the cages as well as thermal and repulsion expansion at higher temperatures and at relatively high hydrogen loadings. At temperatures of 250 K and above it is clear that the mobility of the hydrogen molecules is considerably less restricted particularly for high hydrogen loadings in the small cages and diffusion more rapidly approaches the Fickian limit at shorter times. This is also seen in the estimates for the hydrogen diffusivities (Table IV) which display a dramatic increase with

temperature at high hydrogen occupancy within the smaller cages. These observations are believed to be largely related to an induced melting process at high cage loadings.

As reported by Gorman *et al* [21], the number of inter-cage migration events counted over 0.5 ns simulations were observed to exhibit Arrenhius-like behaviour with activation energies of 21.2 and 25.6 kJ mol^{-1} for 2S1L and 2S4L systems, with respective 95% confidence intervals of ±6.2 and 7.6 kJ mol^{-1}. In this study, *de facto* energy barriers for self-diffusivity *D* were estimated assuming approximate Arrhenius behaviour. As demonstrated in Figs. 8 to 11, Arrhenius fits to *D* for pure systems were superior to those for mixed systems. We believe the primary reason for this is simply that in the pure systems, where more hydrogen molecules are present than in mixed system at the same small-cage occupation, the MSD of the hydrogen molecules is calculated more accurately due to the greater number of samples available. The r^2 values of the Arrhenius fits are provided in Table V, with the resultant activation energies in Table VI; clearly, from inspection of the r^2 values for the mixed systems, especially at lower small-cage occupation, a greater level of statistical sampling is desirable.

[insert Tables V and VI about here]

In the mixed systems, the activation energy increases steadily with small-cage hydrogen occupation, which is not unexpected because the higher the hydrogen occupation, the more difficult it is to hop between the small cages. Moreover, as implied by the results for the singly occupied small cage system, 1S1L, (see Fig. 5) one would expect the activation energy for hopping in the mixed 1S1L system to be quite large leading to a minimum in the activation energy at an intermediate small cage loading and this is inferred to some extent by the results for the pure systems. The relatively high energy barrier in 1S4L may be rationalised by hydrogen hopping events between the small cages being highly dependent on more vigorous vibration of quadruply-occupied large cages and occasional hopping from these into small cavities. For intermediate

loadings in the small cages where a proportion of the small cavities are doubly occupied from the outset, hydrogen hopping between the small cavities is easier, due to repulsions of two hydrogen molecules allowing easier passage into neighbouring singly-occupied cavities. This does lead to a lower activation energies for the intermediate loading systems which are not inconsistent with the results for the mixed systems. (The 1.5S4L system needs to be checked. The D value appears abnormally low at 200K and if the two higher temperatures are omitted for reasons similar to the 1.75S4L and 2S4L runs then an activation energy ~ 18 kJ/mol is obtained which is more physically consistent). Finally, as all small cages are doubly occupied in 2S4L, the activation energy barriers to move to other small cavities again increases due to increased H_2-H_2 repulsion.

CONCLUSIONS

In this work, diffusive transport of hydrogen in clathrates, both pure and mixed (THF+H_2), has been investigated and a mathematical model has been proposed to describe the diffusion process through cage-hopping and anomalous movements within the cavities. The basis for this model is the combination of two different transport modes together. Firstly, the motion of a random-walker within disordered media can be described as anomalous superconducting diffusion which exists over tens of picoseconds under non-percolating conditions. Secondly, a Fickian diffusion process takes place at long times via cage-hopping, which can be represented by the Einstein equation for the mean-square displacement.

The existence of the two modes has been validated by non-linear regression fitting of the MSD of the centre-of-mass of the hydrogen molecules. The two primary parameters, the average range of displacement of the molecule under non-percolating conditions, ℓ, and the long-time Fickian diffusivity, *D*, computed from the nonlinear regression analysis provide insights into the manner in which H_2 may be stabilised with the hydrate structure. For pure H_2 systems below the hydrate melting point the cage sizes within the hydrate systems are comparatively insensitive to hydrogen loading and the activation energies for Fickian diffusion at long times are generally larger in the

pure systems compared to the mixed (H_2-THF) hydrates. In the latter case the magnitude of ℓ, which is indicative of the size/shape of the small cages of the hydrate where the hydrogen is primarily located, is sensitive to loading, increasing as the cage occupancy increases. Interestingly, and consistent with the greater thermodynamic stability of the mixed hydrate relative to the pure H_2 hydrate, the diffusivities of hydrogen in the mixed hydrate are up to an order of magnitude smaller than for the pure system.

ACKNOWLEDGEMENTS

This work was conducted with the support of Science Foundation Ireland (SFI) Grant No. [07/SRC/B1160].

REFERENCES

1. Y.F. Makogon, *Hydrates of Hydrocarbons*, PennWell Books, Tulsa, Oklahoma, 1997.
2. E.D. Sloan and C.A. Koh, *Clathrate Hydrates of Natural Gases*, 3rd rev. ed., CRC Press, Taylor & Francis USA, 2007.
3. G.A. Jeffrey and R.K. McMullan, *Prog. Inorg. Chem.*, 1967, **8**, 43.
4. W.L. Mao, H. Mao, A.F. Goncharov, V.V. Struzhkin, Q. Guo, J. Hu, J. Shu, R.J. Hemley, M. Somayazulu and Y. Zhao, *Science*, 2002, **297**, 2247.
5. S. Patchkovskii and J.S. Tse, *PNAS*, 2003, **100**, 14645-14650.
6. M.H.F Sluiter, H. Adachi, R.V. Belosludov, V.R. Belosludov and Y. Kawazoe, *Mater. Trans.*, 2004, **45**, 1452.
7. S. Alavi, J.A. Ripmeester and D.D. Klug, *J. Chem. Phys*, 2005, **123**, 024507.
8. H. Lee, J. Lee, D.Y. Kim, J. Park, Y.T. Seo, H. Zeg, I.L. Moudrakovski, C.I. Ratcliffe and J.A. Ripmeester, *Nature*, 2005**, 434**, 743.
9. R.V. Belosludov, O.S. Subbotin, H. Mizuseki, Y. Kawazoe and V.R. Belosludov, *J. Chem. Phys.*, 2009**, 131**, 244510.
10. H. Erfan-Niya, H. Modarress and E. Zaminpayma, *J. Incl. Phenom. Macrocycl. Chem.*, 2011**, 70**, 1-2, 227-239.
11. L.J. Florusse, C.J. Peters and J. Schoonman, et al., *Science*, 2004, **306**, 469-471.
12. E. Newson, TH. Haueter, P. Hottinger, F. Von Roth, G.W.H. Schere and TH.H.Schucan. *Inter. J. Hydrogen Energy 23*, 1998, **10**, 905-909.
13. L.J. Rovetto, T.A. Strobel, K.C. Hester, S.F. Dec, C.A. Koh, K.T. Miller and E.D. Sloan, *FY Annual Progress Report*, 2006.
14. T. Nakayama, S. Tomura, M. Ozaki, R. Ohmura and Y.H. Mori, *Energy Fuels*, 2010, 24, 2576–2588.
15. Rovetto, L.J. et al. (2006) 'Molecular hydrogen storage in novel binary clathrate hydrates at near-ambient temperatures and pressures', FY 2006 Annual Progress Report
16. B. Peters, N.E.R. Zimmermann, G.T. Beckham, J.W. Tester and B.L. Trout, *J. Am. Chem. Soc*, 2008, **130**, 17342-17350.
17. A. Demurov, R. Radhakrishnan and B.L. Trout, *J. Chem. Phys.*, 2002, **116**, 702-709.
18. S. Alavi and J.A. Ripmeester, *Angew. Chem. Int. Ed.*, 2007, **46**, 6102.
19. S. Alavi and J.A. Ripmeester, *Chem. Phys. Lett.*, 2009, **479**, 234.
20. T.J. Frankcombe and G.-J. Kroes, *J. Phys. Chem. C*, 2007, **111**, 13044.
21. Gorman, P.D., English, N.J. and MacElroy, J.M.D. (2012), *J. Chem. Phys.* 136(4):044506

22. D. Saha and S. Deng, *Langmuir*, 2010, **26**, 8414-8418.

23. T. Okuchi, M. Takigawa, J. Shu, H.-K. Mao, R.J. Hemley and T. Yagi, *Phys. Rev. B*, 2007, **75**, 144104.

24. L. Senadheera and M.S. Conradi, *J. Phys. Chem. B*, 2008, **112**, 13695.

25. T.Okuchi, I.L. Moudrakovski and J.A. Ripmeester, *Appl. Phys. Lett.*, 2007, **91**, 171903.

26. F.M. Mulder, M. Wagemaker, L. van Eijck and G.J. Kearley, *ChemPhysChem*, 2008, **9**, 1331.

27. T.C. McDermott, T. Akter, J.M.D. MacElroy, D.A. Mooney, M.T.P. McCann, and D.P. Dowling, *Langmuir,* 2012, **28**, 506.

28. D. Lee, L. Zhang, S.T. Oyama, S. Niu and R.F. Saraf, *J. Membr .Sci.***,** 2004, **231**, 117.

29. L. Cuffe, L., J.M.D. MacElroy, M. Tacke, M. Kozachok and D.A. Mooney, *J. Membr. Sci.*, 2006, **272**, 6.

30. S. Araki, N. Mohri, Y. Yoshimitsu, and Y. Miyake, *J. Membr .Sci.***,** 2007, **290**, 138.

31. J.D. Bernal and R.H. Fowler, *J. Chem. Phys.*, 1933, **1**, 515.

32. A. Rahman and F.H. Stillinger, *J. Chem. Phys.*, 1972, **57**, 4009-4017.

33. J. L. F. Abascal and C. Vega, *J. Chem. Phys.*, 2005, 123, 234505.

34. S. Alavi, J.A. Ripmeester and D.D. Klug, *J. Chem. Phys.*, 2006, **124**, 014704.

35. W. Smith, T.R. Forester and I.T. Todorov, 'DL_POLY_2' software, Daresbury Laboratory, Warrington, Great Britain (2006)

36. D.C. Rapaport, *The Art of Molecular Dynamics Simulation,* Second Edition, Cambridge, 2005.

37. U. Essmann, L. Perera, M.L. Berkowitz, T. Darden, H. Lee and L.G. Pedersen, *J. Chem. Phys.*, 1995, **103**, 8577-8595.

38. T. F. Miller, M. Eleftheriou, P. Pattnaik, A. Ndirango, D. Newns and G. J. Martyna, *J. Chem. Phys.*, 2002, **116**, 8649-8659.

39. M.P. Allen and D.J. Tildesley, *Computer Simulation of Liquids,* Oxford, 1987.

40. W.G. Hoover, *Phys. Rev. A*, 1985, **31**, 1695-1697.

41. H.C. Andersen, *J. Chem. Phys.*, 1980, **71**, 2384-2393.

42. W.G. Hoover, *Phys. Rev. A*, 1986, **34**, 2499-2500.

43. Press, W.H.; Teukolsky, S.A.; Vetterling, W.T.; Flannery, B.P. *Numerical Recipes in Fortran 77. The Art of Scientific Computing, 2nd Edition*, Cambridge, 1992

44. Kappel,F. and Kuntsevich, A.V., *Computational Optimisation and Applications*, 15(2):193-205 (2000)

45. Coleman, T.F. and Y. Li(1996), *SIAM Journal on Optimisation*, 6(2):418-445

46. Coleman, T.F. and Y. Li (1994), *Mathematical Programming*, 67(2):189-224, 1994.

47. L.S. Lasdon, A.D. Waren, A. Jain and M. Ratner, ACM Trans. Math Software, 4, 34-50 (1978).

48. Microsoft (2012), *About Solver* Available at: http://office.microsoft.com/en-us/excel-help/about-solver-HP005198368.aspx (Accessed 12th November 2012)

49. Kappel,F.and Kuntsevich, A.V. (1997) *Solvopt*. Available at: http://www.uni-graz.at/imawww/kuntsevich/solvopt (Accessed 12th November 2012)

50. Havlin, S. and Ben-Avraham, D. *Advances in Physics*, **51(1)**, 187-292 (2002)

51. Supplementary Information containing MATLAB Lsqcurvefit and Microsoft EXCEL results for *A*, *l* and *D*

52. P.D. Gorman, N.J. English and J.M.D. MacElroy, *Phys. Chem. Chem. Phys.* **13**, 19780 (2011)

53. N. Varini, N.J. English and C. Trott, *Energies*, **5**, 3526 (2012)

Table I. The ten systems used and naming conventions thereof

1S1L	**1S4L**
128 H_2 in 128 small cages 64 THF in 64 large cages	128 H_2 in 128 small cages 256 H_2 in 64 large cages, 4 in each
1.25S1L	**1.25S4L**
160 H_2 in 128 small cages: ¼ of the small cages doubly occupied by H_2 64 THF in 64 large cages	160 H_2 in 128 small cages, ¼ of the small cages doubly occupied by H_2 256 H_2 in 64 large cages, 4 in each
1.5S1L	**1.5S4L**
192 H_2 in 128 small cages: ½ of the small cages doubly occupied by H_2 64 THF in 64 large cages	192 H_2 in 128 small cages, ½ of the small cages doubly occupied by H_2 256 H_2 in 64 large cages, 4 in each
1.75S1L	**1.75S4L**
224 H_2 in 128 small cages, ¾ of the small cages doubly occupied by H_2 64 THF in 64 large cages	224 H_2 in 128 small cages, ¾ of the small cages doubly occupied by H_2 256 H_2 in 64 large cages, 4 in each
2S1L	**2S4L**
256 H_2 in 128 small cages, 2 in each 64 THF in 64 large cages	256 H_2 in 128 small cages, 2 in each 256 H_2 in 64 large cages, 4 in each

Table II. Results for *A* Calculated by SOLVOPT

Fitting Parameter A						
	200 K	220 K	230 K	240 K	250 K	260 K
1S4L	6.76±0.32	4.359±0.234	3.321±0.46	4.145±0.399	4.63±0.565	7.523±3.74
1.25S4L	2.519±0.091	3.007±0.060	5.832±0.187	3.322±0.090	4.588±0.107	1.657±0.040
1.5S4L	1.907±0.035	2.001±0.034	2.129±0.031	4.158±0.174		
1.75S4L	0.962±0.0075	1.507±0.015	2.305±0.045	1.079±0.012		
2S4L	0.875±0.0086	1.331±0.016	0.803±0.0086	0.641±0.0173		
1.25S1L	0.130±0.0013	0.172±0.0070	0.194±0.0057	0.205±0.0011	0.316±0.0066	0.213±0.0024
1.5S1L	0.163±0.0009	0.245±0.0032	0.203±0.0023	0.247±0.0031	0.274±0.0016	0.267±0.0032
1.75S1L	0.130±0.0016	0.214±0.0013	0.300±0.0017	0.277±0.0020	0.378±0.0039	0.639±0.0041
2S1L	0.182±0.0017	0.198±0.0008	0.245±0.0022	0.323±0.0046	0.454±0.0042	0.773±0.0077

Table III. Results for *l* (Å) calculated by SOLVOPT

Fitting Parameter l (Å)						
	200 K	220 K	230 K	240 K	250 K	260 K
1S4L	0.534±0.0005	0.543±0.0005	0.530±0.0010	0.541±0.0004	0.541±0.0004	0.531±0.0010
1.25S4L	0.566±0.0010	0.57±0.0005	0.561±0.0004	0.578±0.0006	0.577±0.0004	0.635±0.0014
1.5S4L	0.562±0.0006	0.585±0.0007	0.594±0.0005	0.573±0.0007		
1.75S4L	0.603±0.0007	0.604±0.0006	0.587±0.0007	0.706±0.0013		
2S4L	0.585±0.0008	0.595±0.0007	0.747±0.0020	0.917±0.0115		
1.25S1L	0.486±0.0032	0.365±0.0004	0.403±0.0035	0.483±0.0014	0.407±0.0016	0.627±0.0047
1.5S1L	0.439±0.0010	0.43±0.0015	0.521±0.0028	0.486±0.0020	0.528±0.0011	0.596±0.0033
1.75S1L	0.625±0.0090	0.677±0.0033	0.775±0.0033	0.73±0.0036	0.748±0.0041	2.366±0.077
2S1L	0.459±0.0017	0.857±0.0053	0.771±0.0062	0.729±0.0061	1.272±0.017	2.933±0.045

Table IV. Results for D (10^{-12} m^2/s) calculated by SOLVOPT

Fitting Parameter D, (*10^(-12)m2/s)						
	200 K	220 K	230 K	240 K	250 K	260 K
1S4L	0.31±0.0098	2.494±0.012	4.522±0.023	5.175±0.011	9.218±0.009	15.25±0.026
1.25S4L	2.814±0.0215	6.482±0.010	8.615±0.009	14.4±0.014	14.41±0.009	27.64±0.031
1.5S4L	0.784±0.0134	5.093±0.014	7.295±0.012	11.724±0.017		
1.75S4L	5.597±0.013	12.551±0.012	16.565±0.014	37.04±0.029		
2S4L	1.46±0.015	16.446±0.015	32.488±0.039	46.263±0.210		
1.25S1L	0.447±0.0254	2.905±0.037	3.938±0.035	3.032±0.014	4.865±0.014	3.456±0.048
1.5S1L	1.076±0.0093	2.844±0.017	2.47±0.028	4.09±0.023	5.764±0.023	8.801±0.039
1.75S1L	2.216±0.0651	3.120±0.033	4.028±0.039	8.72±0.042	12.68±0.042	32±0.716
2S1L	1.236±0.0168	1.911±0.044	3.946±0.065	10.1±0.078	29.92±0.078	78.7±0.662

Table V. The coefficient of determination of Arrhenius fits to D

Systems	Coefficient of Determination
1.25S1L	0.703
1.5S1L	0.93
1.75S1L	0.87
2S1L	0.88
1S4L	0.97
1.25S4L	0.97
1.5S4L	0.99
1.75S4L	0.94
2S4L	0.97

Table VI. The activation energy derived from Arrhenius fits to D, with 95% confidence intervals

Activation Energy, in kJ/mol			
		1S4L	26.73±6.84
1.25S1L	14.54±13.11	1.25S4L	15.57±3.60
1.5S1L	14.23±4.69	1.5S4L	27.41±4.43
1.75S1L	18.51±10.42	1.75S4L	17.58±12.9
2S1L	30.34±15.4	2S4L	35.56±19.16

Figure Captions

Figure 1. Schematic showing the general features of the MSD of H_2 in a clathrate (log-log plot).

Figure 2. Mean square displacement (MSD) of hydrogen molecules within clathrate hydrates for the 2S4L system: ■,200K; ◆,220K; □,230K; ◇240K. The calculated MSDs (500 ps from 2.5 ns, 1000 points) are shown as the long dashed curves and the non-linear fits using eqn. 3 are shown as solid lines in each case.

Figure 3. MSD of hydrogen molecules for the 2S1L system: ■, 200 K; ◆, 220 K; □, 230 K; ◇, 240 K; ○, 250 K; ●, 260 K. Otherwise, as in Fig. 2.

Figure 4 MSD of hydrogen molecules for the 1S4L system: ■, 200 K; ◆, 220 K; □, 230 K; ◇, 240 K; ○, 250 K; ●, 260 K. Otherwise, as in Fig. 2.

Figure 5. The MSD curve for 1S1L at 260 K. The full MSD is shown as the red dashed curve and the non-linear fit by the solid blue line. Hopping was not observed.

Figure 6. Example of the deconvolution of MSD based on eqn. 3 at 200 K for 1.25S1L system.

Figure 7. Example of the deconvolution of MSD based on eqn. 3 at 260 K for 1.25S1L system.

Figure 8. Arrhenius plots of the diffusion coefficient within the stable temperature range for the systems of 1S4L, 1.25S4L and 1.75S4L.

Figure 9. Arrhenius plots of the diffusion coefficient within the stable temperature range for the systems of 1.5S4L and 2S4L.

Figure 10. Arrhenius plots of the diffusion coefficient within the stable temperature range for the systems of 1.25S1L and 1.75S1L.

Figure 11. Arrhenius plots of the diffusion coefficient within the stable temperature range for the systems of 1. 5S1L and 2S1L.

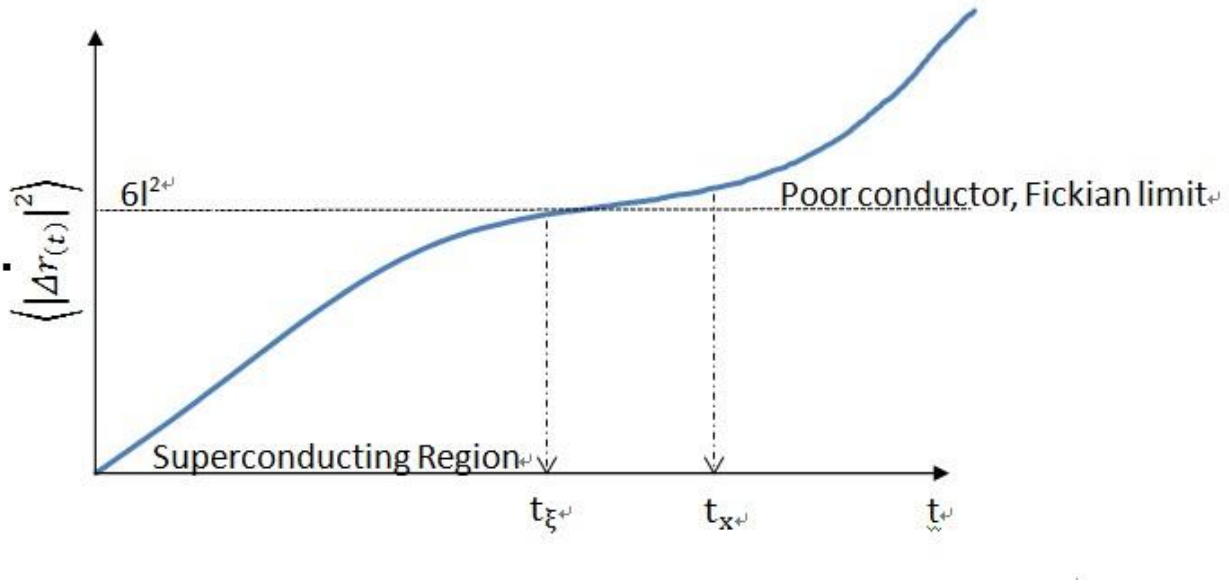

Figure 1

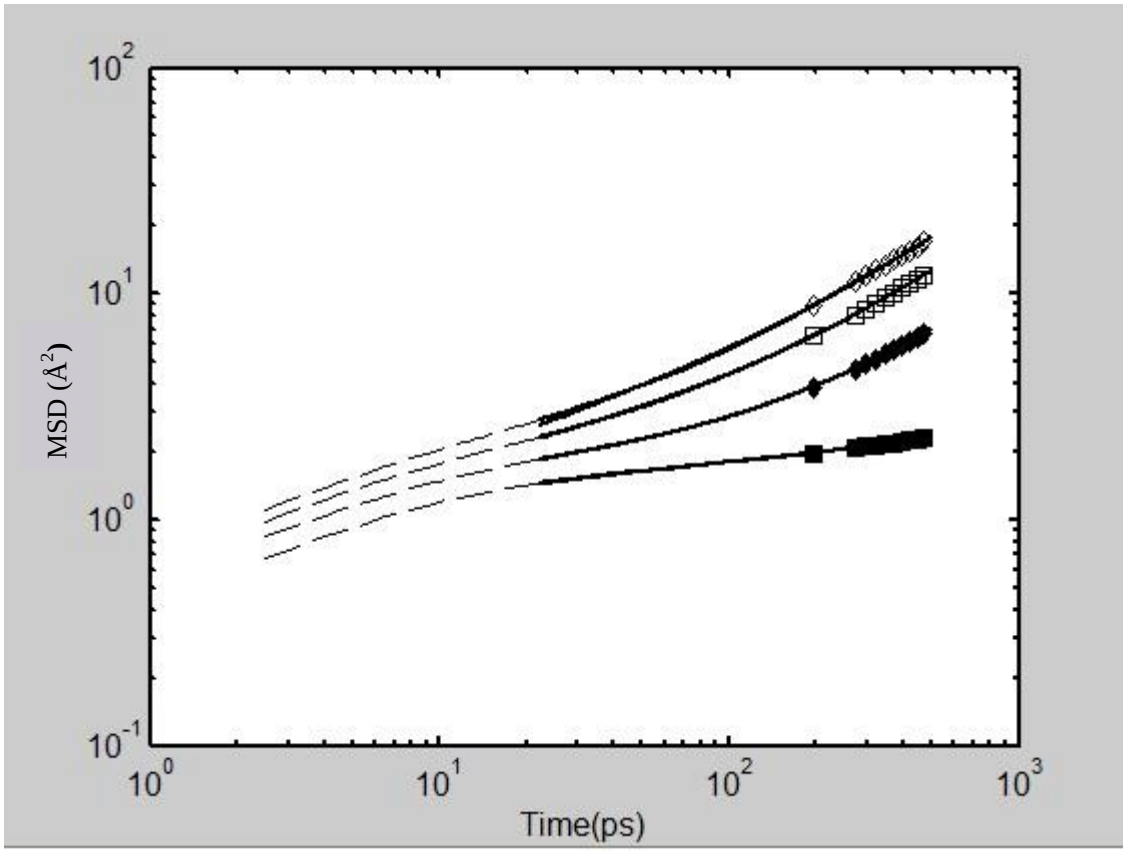

Figure 2

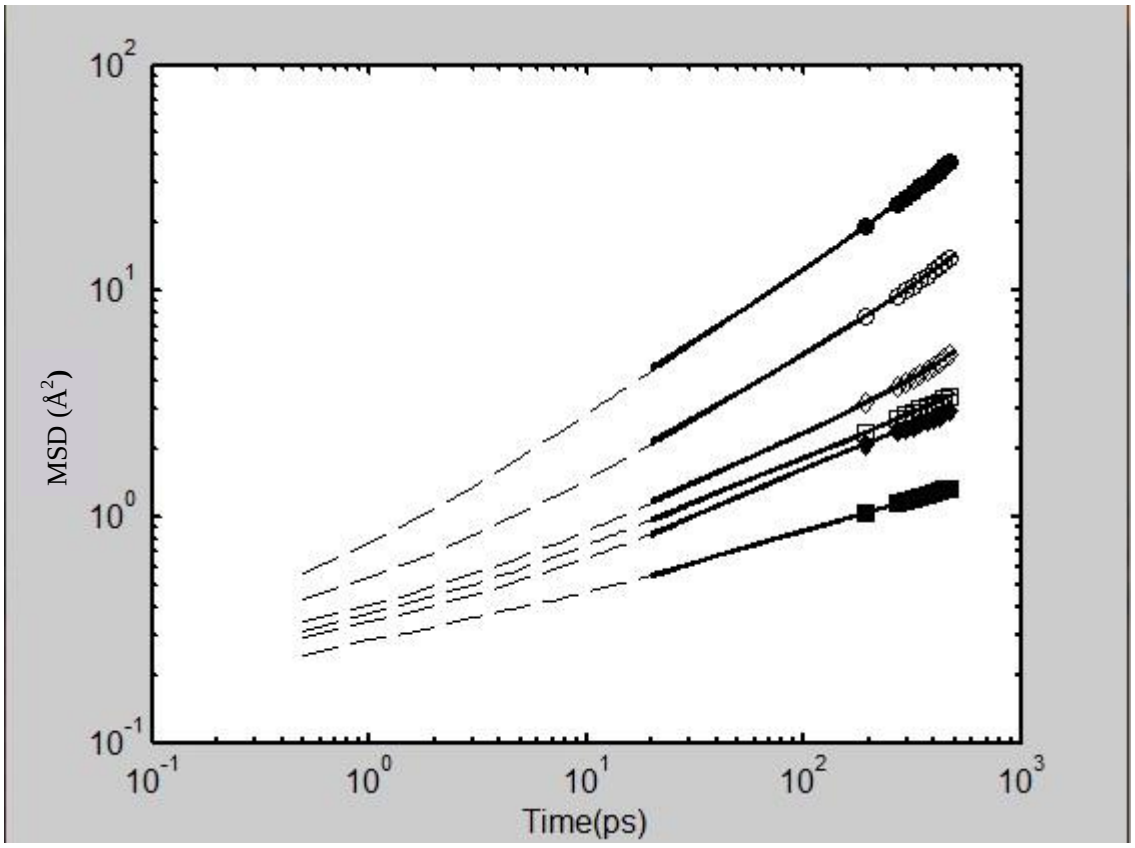

Figure 3

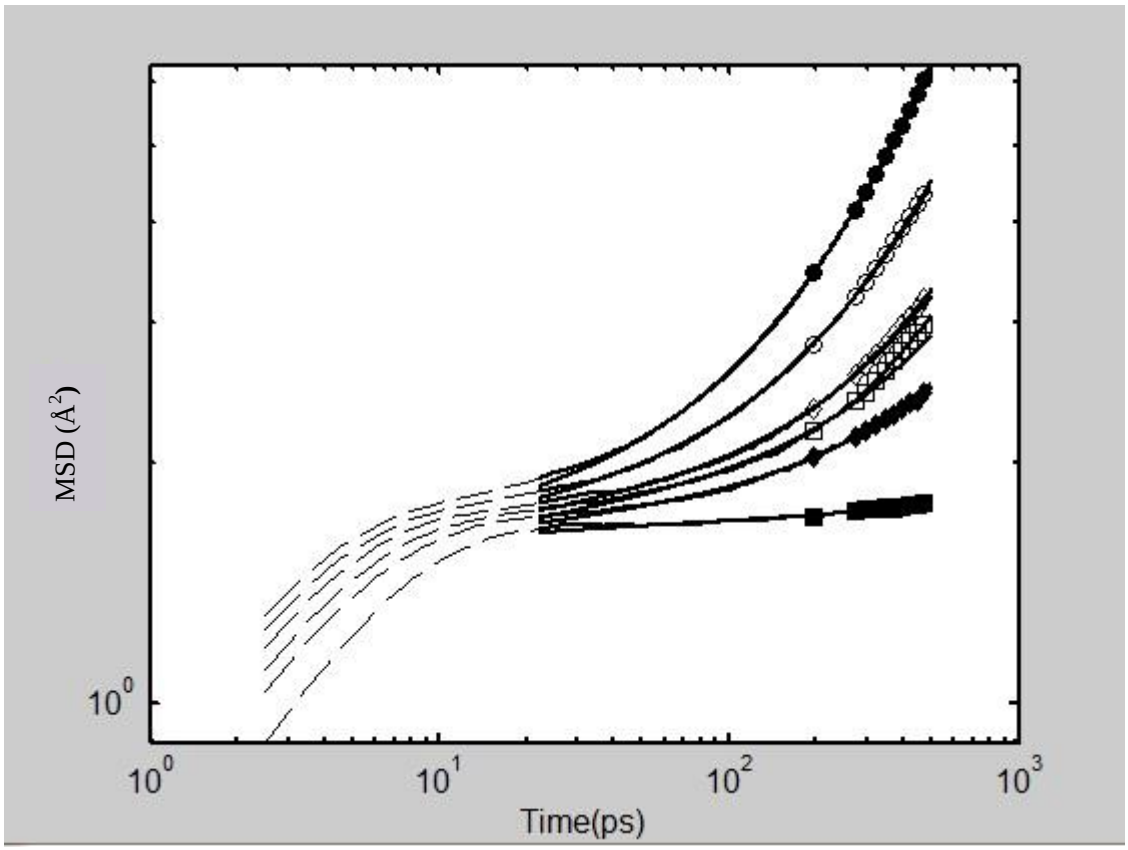

Figure 4

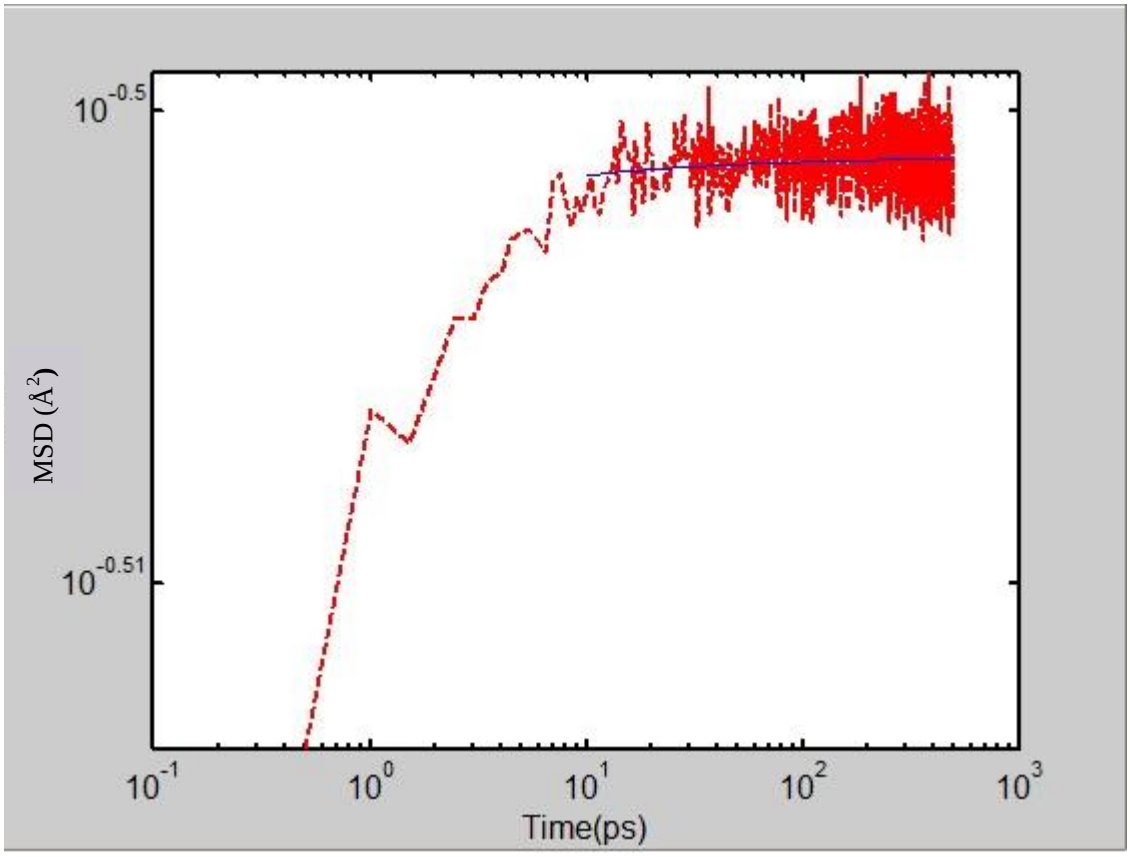

Figure 5

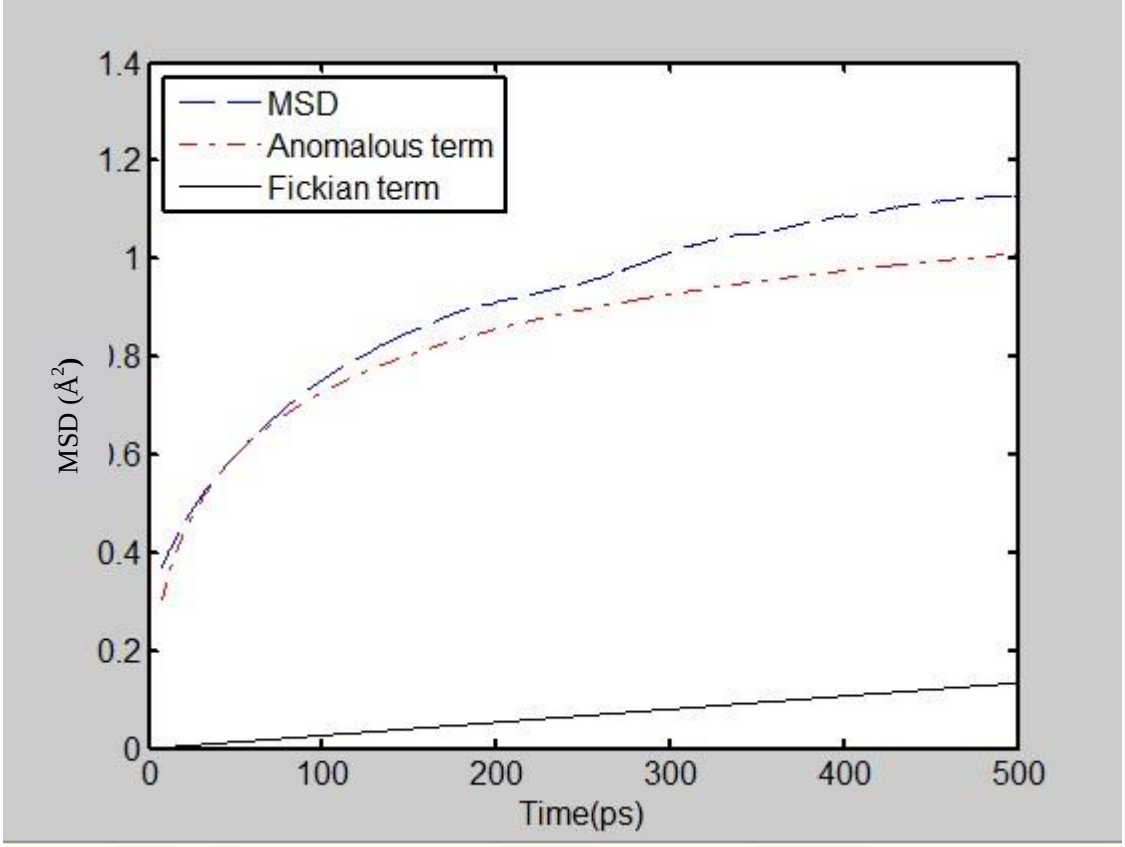
MSD
Anomalous term
Fickian term
MSD (Å²)
Time(ps)
0
0.2
0.4
.6
.8
1
1.2
1.4
0
100
200
300
400
500

Figure 6

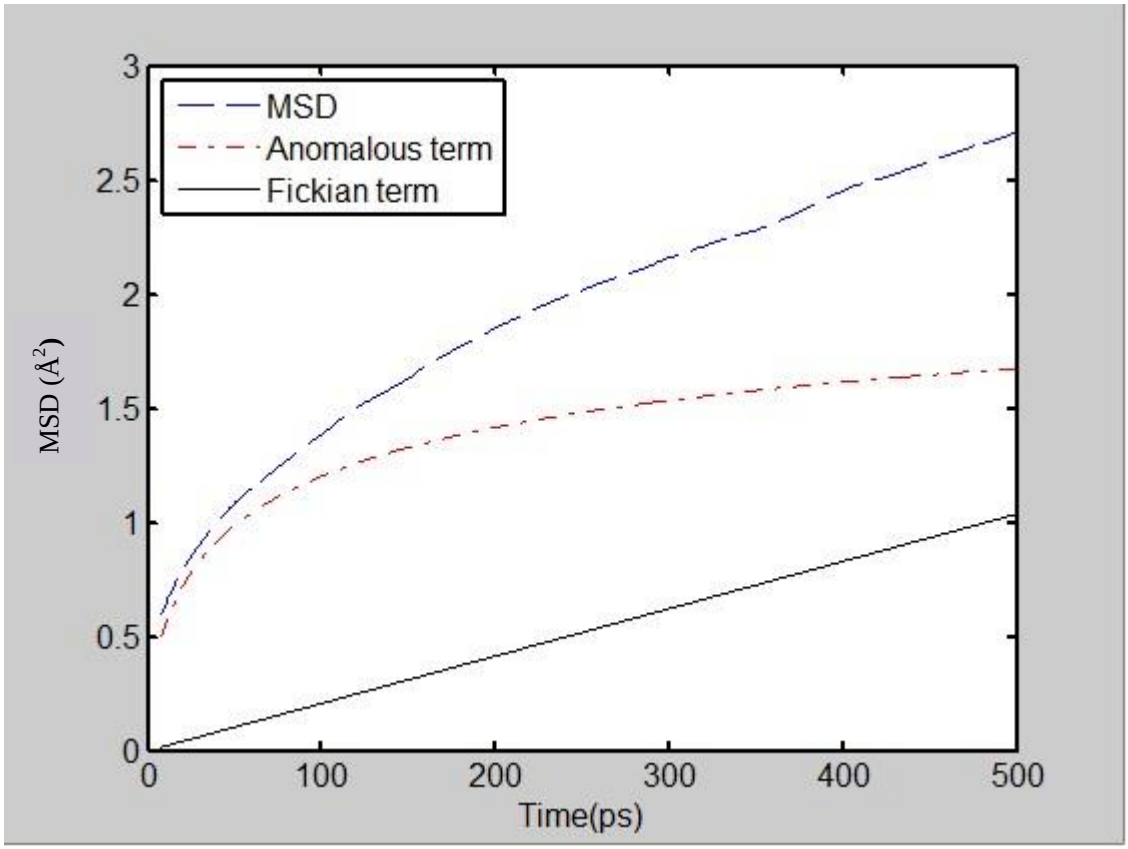
MSD
Anomalous term
Fickian term
MSD (Å²)
Time(ps)
0
0.5
1
1.5
2
2.5
3
0
100
200
300
400
500

Figure 7

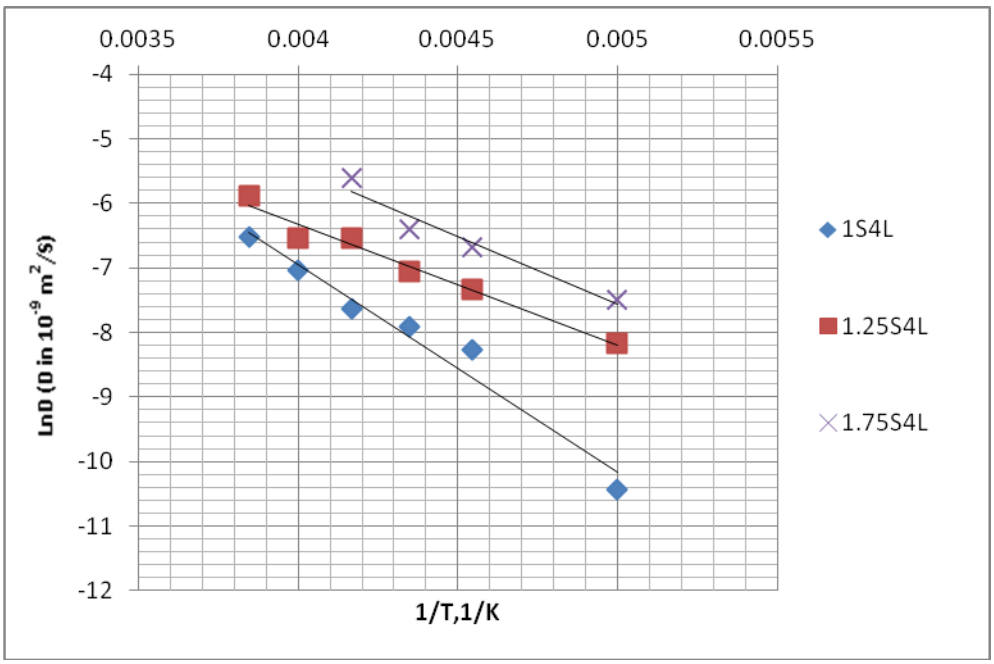

Figure 8

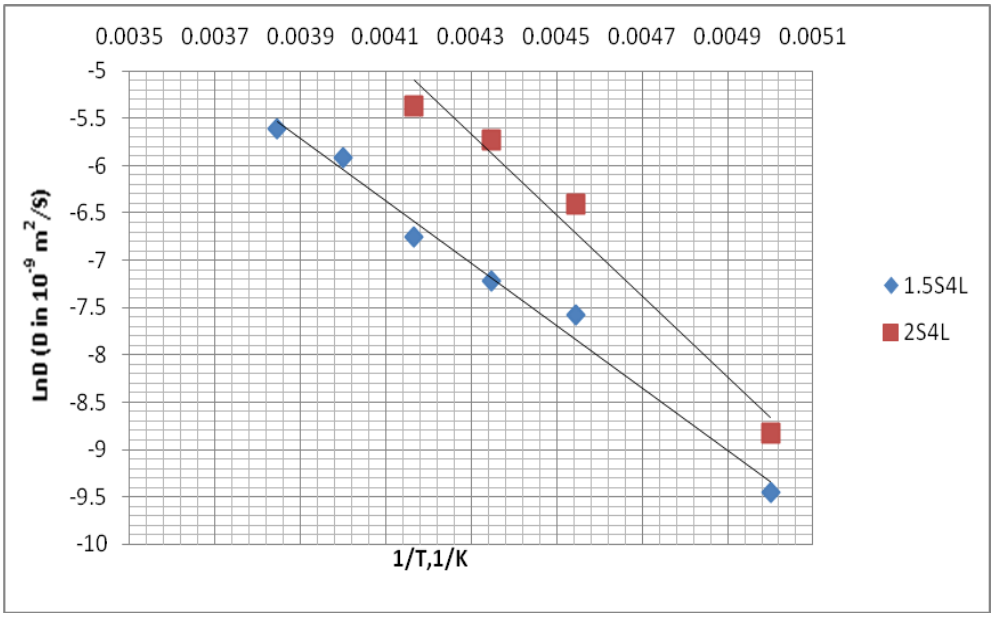

Figure 9

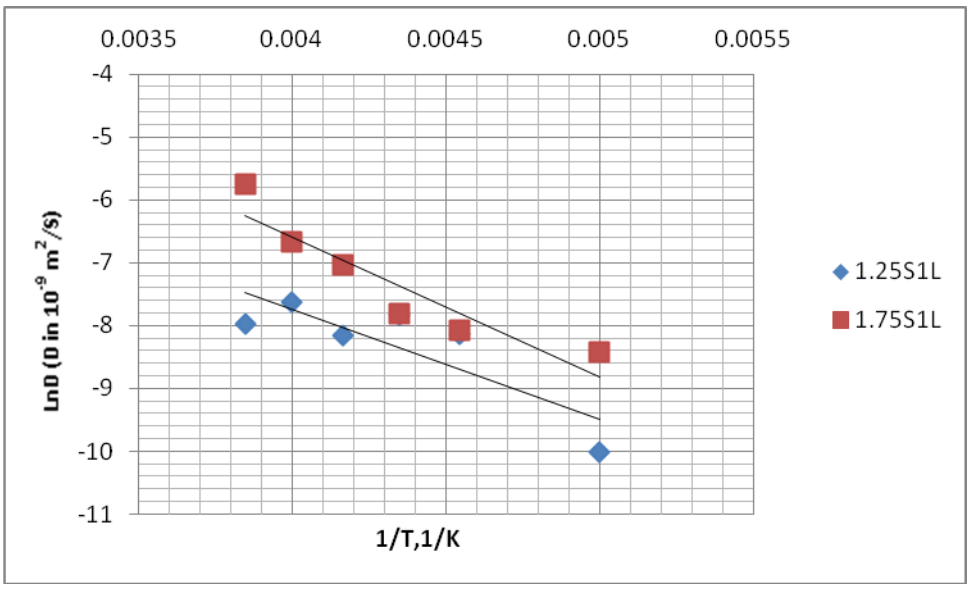

Figure 10

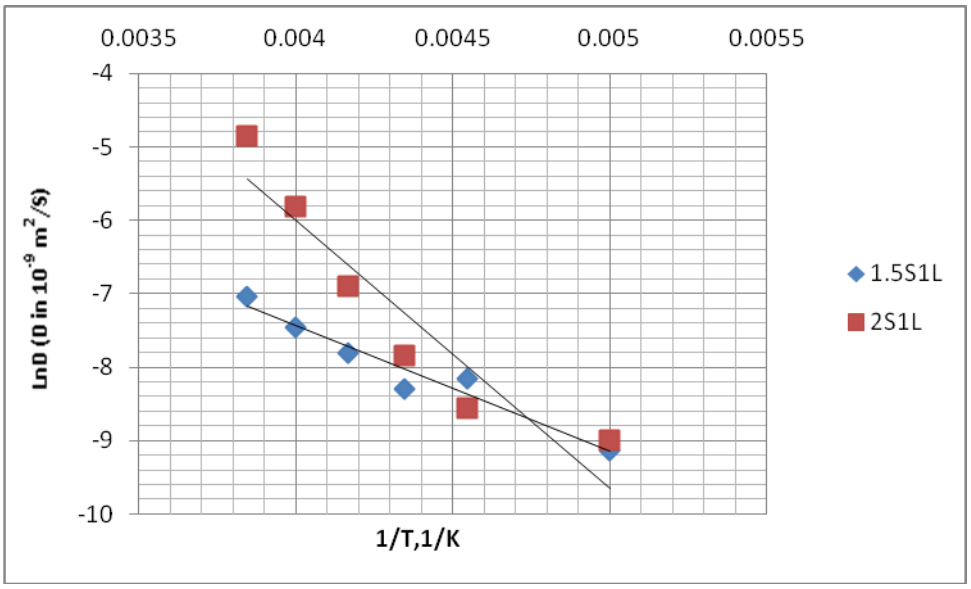

Figure 11